

Size selection and stability of thick-walled vesicles

M.J. Greenall^{a*}

^aSchool of Mathematics and Physics, University of Lincoln, Brayford Pool, Lincoln, LN6 7TS, United Kingdom

In recent experiments, small, thick-walled vesicles with a preferred size were formed from copolymers where the degree of polymerisation of the hydrophobic block, N_B , was significantly greater than that of the hydrophilic block, N_A . We show that a simple mean-field theory can reproduce several aspects of the behaviour of these vesicles. Firstly, we find a minimum in the free energy of the system of vesicles as a function of their radius, corresponding to a preferred size for the vesicles, when N_B is several times larger than N_A . Furthermore, the vesicle radius diverges as N_B is increased towards a critical value, consistent with the instability of the vesicles with respect to further aggregation seen in the experimental work. Finally, we find that this instability can also be triggered in our model by changing the interaction strength of the copolymers with the solvent.

I. INTRODUCTION

Amphiphiles such as lipids and block copolymers can self-assemble into a range of aggregates in a solvent¹. Some of these structures, known as *micelles*, consist of a hydrophobic core surrounded by a hydrophilic corona. Micelles may be spherical or worm-like in shape². Other aggregates, called *vesicles*, are bag-like structures formed of a *bilayer* of amphiphiles, and enclose a volume of solvent. Although vesicles are often roughly spherical³, their underlying physics differs from that of spherical micelles. In particular, the radius of a spherical micelle can be predicted from the architecture and interactions of the amphiphiles^{4,5}. However, the size of a vesicle is often determined by other factors. In systems containing only one type of simple amphiphile (such as a lipid or diblock copolymer), the effect that limits the growth of self-assembled vesicles is often their translational entropy^{6,7}. The resulting vesicle size distribution is often broad^{8,9} and depends sensitively on the amphiphile concentration¹⁰. In practice, control over the size of vesicles is often obtained by filtration¹¹ or by using a more complex preparation method, such as dewetting from a template¹². The possibility also exists of mixing two types of amphiphile¹³, which divide unevenly between the inner and outer leaflets of the membrane and give the vesicle a preferred size.

However, in recent experiments performed by Warren et al³, vesicles with a narrow size distribution have been formed in a solution of a single type of diblock copolymer by self-assembly. Vesicles with comparable size distributions were formed by two different pathways: polymerisation-induced self-assembly (PISA), where polymerisation continues after self-assembly has started, and rehydration of a thin copolymer film³. This suggests that a suspension of vesicles of a well-defined size is the equilibrium phase in this system. These vesicles have two distinguishing features. Firstly, they are formed of highly asymmetric polymers, with the degree of polymerisation of the hydrophobic block as high as 15 times that of the hydrophilic block³. Secondly, the walls of the vesicles are thick, and their thickness is often of the order of magnitude of the radius of the central liquid pocket. In this report, we take a first step towards understanding these systems by developing a simple mean-field model that predicts the existence of vesicles with a preferred size for strongly asymmetric copolymers and also reproduces other aspects of the experimental system.

II. MEAN-FIELD MODEL

Mean-field models have been used to study spherical micelles in solution^{5,14,15}, and have also been applied to cylindrical micelles¹⁶ and flat bilayers¹⁷. They provide a good description of experimental results on both block copolymers in solution⁴ and block copolymer/homopolymer blends¹⁸. To set up a mean-field model, the principal contributions to the free energy of a system of micelles (neglecting fluctuations) are identified, and formulas for these are found. For example, the Flory-Huggins expression is used for the free energy of mixing of copolymers and homopolymers outside the micelles⁵. The various terms are then added together, and the resulting expression is minimised. This yields a number of predictions, including the equilibrium radius of the micelles. Here, we apply this approach to a system of spherical vesicles, with the aim of finding whether these aggregates have a preferred radius at equilibrium. The theory will be developed for diblock copolymers formed of N_A A monomers and N_B B monomers mixed with a ‘solvent’ of homopolymers containing N_h A monomers. However, for simplicity, we will set $N_h = 1$ in our numerical calculations.

To begin, we introduce the contributions to the free energy of a single vesicle. The first of these arises from the fact that the copolymers in an aggregate are deformed away from their unperturbed state⁵. This leads to an elastic

energy term for the inner leaflet of the vesicle given by

$$\mathcal{F}_d^{\text{in}} = \frac{3}{2}kTp_1 \left\{ \frac{(R_1 - R_0)^2}{N_A a^2} + \frac{N_A a^2}{(R_1 - R_0)^2} + \frac{(R_2 - R_1)^2}{N_B a^2} + \frac{N_B a^2}{(R_2 - R_1)^2} - 4 \right\}, \quad (1)$$

where k is Boltzmann's constant, T is the temperature, a is the segment length, p_1 is the number of copolymers in the inner leaflet and the R_i are the radii shown in Fig. 1. This term is zero when the polymers are in their unperturbed state and gives an energy penalty when they are stretched or compressed^{5,18,19}. A similar term, $\mathcal{F}_d^{\text{out}}$, exists for the outer leaflet, which contains p_2 copolymer chains.

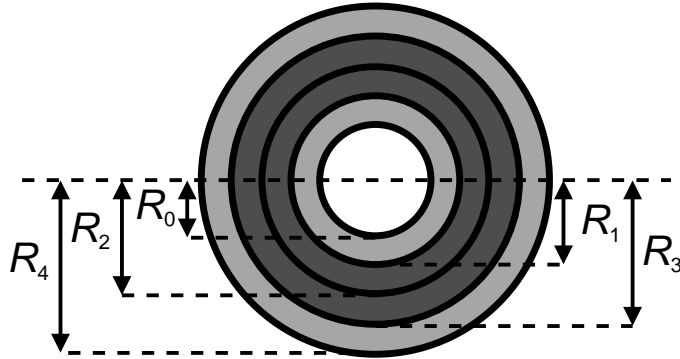


FIG. 1: Geometry of a spherical bilayer vesicle with outer radius R_4 . The dark grey regions are hydrophobic and the light grey regions are hydrophilic. The vesicle is surrounded by solvent and encloses a spherical volume of solvent with radius R_0 in its centre.

The hydrophilic layers of the vesicle (light grey in Fig. 1) are assumed to consist of copolymer A blocks and solvent, and the hydrophobic layers (dark grey in Fig. 1) of copolymer B blocks and solvent. This leads to a term representing the entropy of mixing of the solvent with the copolymer chains⁵, given in the case of a vesicle by

$$\mathcal{F}_m = \sum_{i=1}^4 \frac{4\pi}{3} \frac{R_i^3 - R_{i-1}^3}{a^3} kT \frac{1 - \eta_i}{N_h} \ln(1 - \eta_i). \quad (2)$$

Here, the volume fraction of copolymer in each layer is η_i , where i runs from 1 in the innermost layer to 4 in the outermost layer. By allowing η_2 and η_3 to be less than one, we allow solvent to penetrate into the hydrophobic layers. This is necessary to model the experiments of Warren et al³, where significant ingress of water molecules into the vesicle membrane was observed. Since, in general, $\eta_2 \neq \eta_3$, our model allows for the concentrations of solvent in the inner and outer hydrophobic layers to be different. However, this difference is very small in all stable aggregates.

The solvent has a repulsive interaction with the hydrophobic blocks, whose strength is given by the Flory-Huggins χ parameter. This results⁴ in the following term in the free energy:

$$\mathcal{F}_{\text{core}} = \frac{4\pi}{3} \frac{(R_2^3 - R_1^3)}{a^3} kT \eta_2 (1 - \eta_2) \chi + \frac{4\pi}{3} \frac{(R_3^3 - R_2^3)}{a^3} kT \eta_3 (1 - \eta_3) \chi. \quad (3)$$

The vesicle contains two surfaces that separate a hydrophilic region from a predominantly hydrophobic region. Each of these produces a contribution to the free energy of the vesicle proportional to its area and to the square root of the χ parameter^{5,20}:

$$\mathcal{F}_{\text{int}} = 4\pi R_1^2 \frac{kT}{a^2} \sqrt{\frac{\chi}{6}} \eta_2 + 4\pi R_3^2 \frac{kT}{a^2} \sqrt{\frac{\chi}{6}} \eta_3. \quad (4)$$

The factors of η_2 and η_3 arise since the hydrophobic layers contain some solvent, and each term is reduced from the value it would have for an interface between pure hydrophobic and hydrophilic layers⁴. The total free energy of a vesicle is given by the sum of the terms above: $\mathcal{F} = \mathcal{F}_d^{\text{in}} + \mathcal{F}_d^{\text{out}} + \mathcal{F}_m + \mathcal{F}_{\text{int}}$. We also assume that the system is incompressible. This allows us to express the η_i in terms of the copolymer parameters and the dimensions of the vesicle and so reduce the number of variables. For example, in the innermost layer, $\eta_1 = 3p_1 N_A a^3 / [4\pi(R_1^3 - R_0^3)]$.

To calculate the free energy of a system of vesicles, we note that, if Ω is the total number of monomers in the system, ϕ is the volume fraction of copolymers and ζ is the fraction of copolymer chains in aggregates, then the total number of vesicles is given by $\Omega\phi\zeta / [(p_1 + p_2)(N_A + N_B)]$. We can then write the total free energy of the system as

$$F_M = \left\{ \frac{\Omega\phi\zeta}{(p_1 + p_2)(N_A + N_B)} \right\} \mathcal{F} + F_{\text{mix}} - TS_m, \quad (5)$$

where F_{mix} is the free energy of mixing of copolymers and solvent outside the vesicles²¹ and S_{m} is the translational entropy of the ‘gas’ of vesicles⁵. Adapting the expression in Ref. 5 to the case of vesicles, we find that the free energy of mixing is given by

$$\frac{F_{\text{mix}}}{kT} = \Omega(1 - \xi\phi\zeta) \left[\frac{\phi_1}{N} \ln \phi_1 + \frac{1 - \phi_1}{N_{\text{h}}} \ln(1 - \phi_1) + \frac{\chi N_{\text{B}} \phi_1}{N_{\text{A}} + N_{\text{B}}} \left(1 - \frac{\phi_1 N_{\text{B}}}{N_{\text{A}} + N_{\text{B}}} \right) \right], \quad (6)$$

where

$$\xi = \frac{1}{(p_1 + p_2)(N_{\text{A}} + N_{\text{B}})} \left(\frac{p_1 N_{\text{A}}}{\eta_1} + \frac{p_1 N_{\text{B}}}{\eta_2} + \frac{p_2 N_{\text{B}}}{\eta_3} + \frac{p_2 N_{\text{A}}}{\eta_4} \right).$$

The factor of $\Omega(1 - \xi\phi\zeta)$ in Eqn. 6 is the total number of monomers outside the vesicles, and $\phi_1 = \phi(1 - \zeta)/(1 - \xi\phi\zeta)$ is the fraction of monomers outside vesicles that belong to copolymers. Similarly, we adapt the lattice model calculation of the translational entropy of micelles in Ref. 5 to the case of vesicles, and find that

$$\frac{S_{\text{m}}}{k} = -\Omega \left\{ \frac{\phi\zeta}{(p_1 + p_2)(N_{\text{A}} + N_{\text{B}})} \ln(\phi\zeta\tilde{\xi}) + \frac{1 - \phi\zeta\tilde{\xi}}{\tilde{\xi}(p_1 + p_2)(N_{\text{A}} + N_{\text{B}})} \ln(1 - \phi\zeta\tilde{\xi}) \right\}, \quad (7)$$

where

$$\tilde{\xi} = 4\pi R_4^3 / [(p_1 + p_2)(N_{\text{A}} + N_{\text{B}})3a^3].$$

The differences with the micelle calculation arise from the existence of the two layers in the vesicle wall and the fact that the central pocket of solvent must be treated as being within the vesicle.

To find whether the vesicles formed from polymers with a given set of values for N_{A} , N_{B} and χ have a preferred size, we first set R_4 to a fixed value and minimise Eqn. 5 with respect to R_0 , R_1 , R_2 , R_3 , p_1 , p_2 and ϕ_1 using a direction set method²². We then repeat the calculation for different values of R_4 to find whether F_{M} has a minimum as a function of R_4 (corresponding to a preferred radius).

III. RESULTS

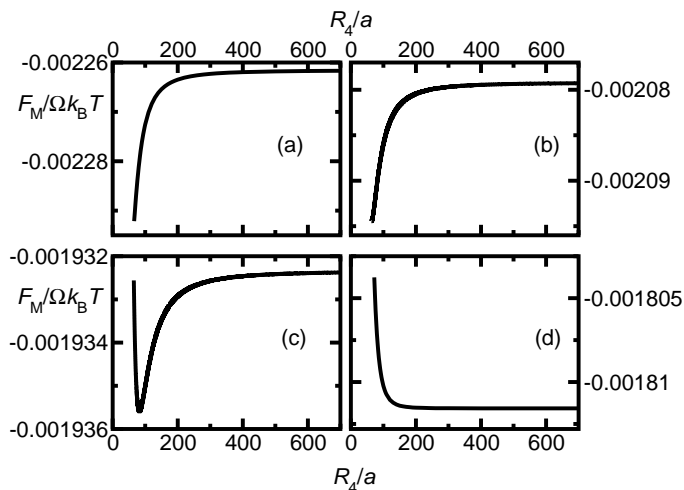


FIG. 2: Total free energy of the system of vesicles versus the outer radius of the vesicle at $N_{\text{A}} = 100$ and (a) $N_{\text{B}} = 300$; (b) $N_{\text{B}} = 350$; (c) $N_{\text{B}} = 400$; (d) $N_{\text{B}} = 450$.

To begin, we focus on a system of relatively short copolymers, and set $N_{\text{A}} = 100$ while varying N_{B} . Since the solvent consists of A monomers (so that $N_{\text{h}} = 1$), we set χ to the relatively high value of 2 to ensure that aggregation takes place over a range of N_{B} . The volume fraction of copolymers is set to $\phi = 0.01$, giving a dilute system. Plots

of $F_M/\Omega k_B T$ are shown in Fig. 2. For $N_B \lesssim 350$, F_M falls monotonically as R_4 decreases, dropping sharply for $R_4 \lesssim 200$. At small values of R_4 , we are no longer able to minimise Eqn. 5. A likely explanation of these results is that the vesicle is unstable with respect to micelle formation. This is borne out by the fact that p_1 shrinks rapidly as R_4 becomes small. In contrast, when $N_B = 400$, a clear minimum is present in the free energy, corresponding to a preferred size for the vesicles. When N_B is increased to 450, the minimum disappears, and F_M decays monotonically as R_4 increases. Here, there is no optimum radius, and the system might either precipitate or form vesicles with a broad size distribution.

Next, we consider longer copolymers, with $N_A = 1000$ and N_B being varied (Fig. 3). Here, the minimum first appears for more strongly asymmetric copolymers, with $N_B \approx 10N_A$, and persists over a wider range of values of N_B . At all free energy minima shown here (and in Fig. 2c above), the vesicles are thick-walled, with a small central solvent pocket. For example, in Fig. 3c, when $N_B = 16000$ the outer radius of the vesicle at the minimum is $R_4 \approx 989a$, while the inner radius is $R_0 \approx 382a$. We note at this stage that the existence of the free energy minimum as a function of the vesicle radius requires tuning of the copolymer parameters to a specific range in which the degree of polymerisation of the hydrophobic block is significantly larger than that of the hydrophilic block. This is in line with the fact that amphiphiles in solution do not generally form vesicles of a preferred size spontaneously²³.

Having found a favoured vesicle size in calculations on two families of copolymers, we now attempt to understand the physical processes that lead to this effect. As R_4 is varied, the contributions to the free energy that vary over

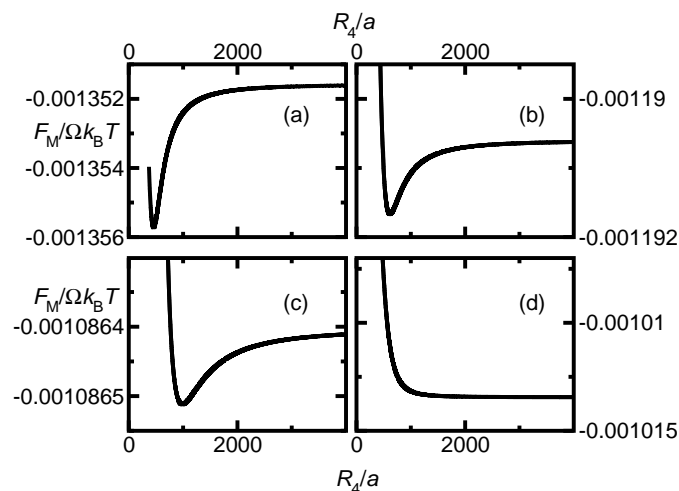


FIG. 3: The total free energy of the system of vesicles as a function of the outer radius of the vesicle at fixed hydrophilic block length $N_A = 1000$ and four different hydrophobic block lengths: (a) $N_B = 10000$; (b) $N_B = 13000$; (c) $N_B = 16000$; (d) $N_B = 19000$.

the largest range are those associated with the individual vesicles, with the bulk contributions changing more slowly. This means that, as for micelles⁵, the equilibrium structure of the vesicle may be found, to a good approximation, by minimising the free energy per chain in the vesicle. Of the terms in the free energy per chain in the vesicle, those that vary most are the free energy of mixing, \mathcal{F}_m , and the surface free energy, $\mathcal{F}_{\text{surf}}$, and these are plotted in Fig. 4 for $N_A = 100$ and a range of values of N_B . We see that the free energy of mixing per chain rises as R_4 is increased for all the values of N_B shown. When $N_B = 100$, the surface free energy per chain also grows as R_4 is increased. However, for $N_B = 400$, it becomes a decreasing function of R_4 . The fall in the surface free energy per chain is very close to the rise in the free energy of mixing per chain, and this fine balance leads to the minimum in F_M in Fig. 2c. In the final case, when $N_B = 500$, the fall in the surface energy is faster, and dominates the rise in the mixing energy, leading to a monotonic decay of F_M with R_4 .

Having identified the change in behaviour of the surface free energy per chain as the mechanism behind the appearance and disappearance of size selection as N_B is increased, we now study this term in more detail and plot the surface free energy and the aggregation number of the vesicle separately in Fig. 5 for copolymers with $N_A = 100$, $N_B = 100$ and $N_A = 100$, $N_B = 500$. As would be expected, $\mathcal{F}_{\text{surf}}$ for the longer copolymers is slightly lower at a given R_4 , as the vesicle walls are thicker and the radius of the inner hydrophobic/hydrophilic interface, R_1 , is smaller. Both curves can be fitted very well by a power law of the form $F_{\text{surf}}/k_B T \sim R_4^\rho$ with $\rho \approx 2.139$ when $N_B = 100$ and $\rho \approx 2.200$ when $N_B = 500$.

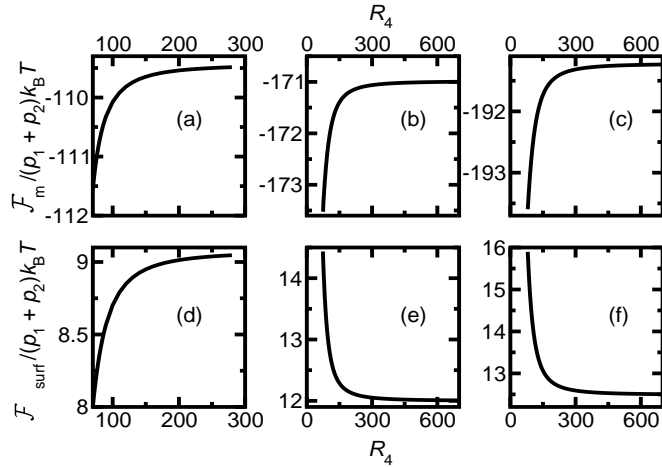


FIG. 4: Top three panels: free energy of mixing per chain in the vesicle versus the vesicle outer radius for (a) $N_A = 100$, $N_B = 100$; (b) $N_A = 100$, $N_B = 400$; (c) $N_A = 100$, $N_B = 500$. Bottom three panels: surface free energy of the vesicle per chain versus the vesicle outer radius for (d) $N_A = 100$, $N_B = 100$; (e) $N_A = 100$, $N_B = 400$; (f) $N_A = 100$, $N_B = 500$.

The difference between the aggregation numbers of the two vesicles is more pronounced, with that of the $N_B = 500$ vesicles being smaller due to the greater volume of the longer molecules. Again, both sets of results can be fitted by a power law, so that $p_1 + p_2 \sim R_4^\sigma$ with $\sigma = 2.137$ when $N_B = 100$ and $\sigma = 2.207$ when $N_B = 500$. The stronger variation when $N_B = 500$ occurs since the bilayers of these vesicles are highly asymmetric at small R_4 , with $p_2 \gg p_1$. As R_4 increases, more molecules enter the inner leaflet, and the asymmetry decreases. In contrast, the $N_B = 100$ vesicles are close to symmetric at smaller values of R_4 and so display a weaker variation of $p_1 + p_2$ with R_4 .

Since $\rho > \sigma$ when $N_B = 100$, but $\sigma > \rho$ when $N_B = 500$, the surface free energy per chain changes from an increasing function of R_4 to a decreasing function as N_B is increased. The fine balance between these terms leads to the appearance of vesicles of a preferred size for a range of $N_B > N_A$, which ultimately become unstable for large N_B .

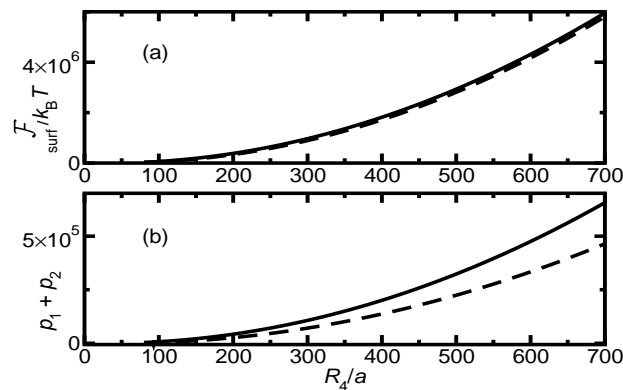


FIG. 5: (a) Vesicle surface free energy versus outer radius for $N_A = 100$, $N_B = 100$ (full line) and $N_A = 100$, $N_B = 500$ (dashed line). (b) Vesicle aggregation number versus outer radius for $N_A = 100$, $N_B = 100$ (full line) and $N_A = 100$, $N_B = 500$ (dashed line).

We now look in more detail at the growth of the vesicle as N_B is increased. In Fig. 6, we plot R_4 against N_B for (a) $N_A = 100$ and (b) $N_A = 1000$. In both cases, the vesicle radius grows slowly at first before diverging as a critical value of N_B . This is consistent with experiments^{2,3}, where the vesicles become unstable above a critical value of N_B .

The instability can also be triggered by a change in χ . In Fig. 7, we plot R_4 against χ for the (a) $N_A = 100$, $N_B = 400$

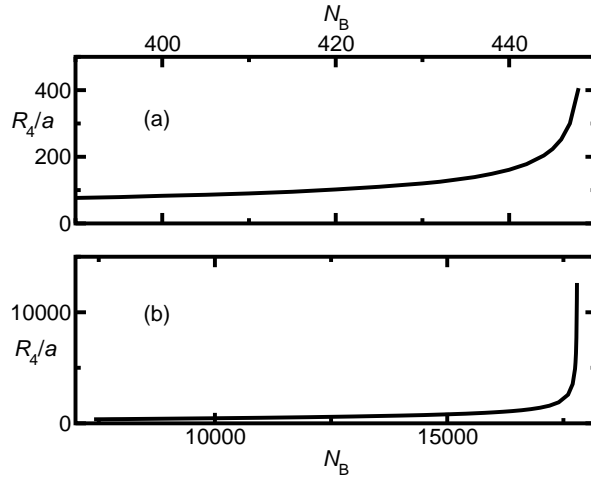


FIG. 6: Outer radius of the vesicle versus the degree of polymerisation of the hydrophobic block for (a) $N_A = 100$ and (b) $N_A = 1000$.

and (b) $N_A = 1000$, $N_B = 13000$ copolymers. The radius is initially relatively insensitive to χ for both copolymers, before diverging sharply at $\chi \approx 3.5$ in the case of the shorter molecules and $\chi \approx 7$ for the longer ones.

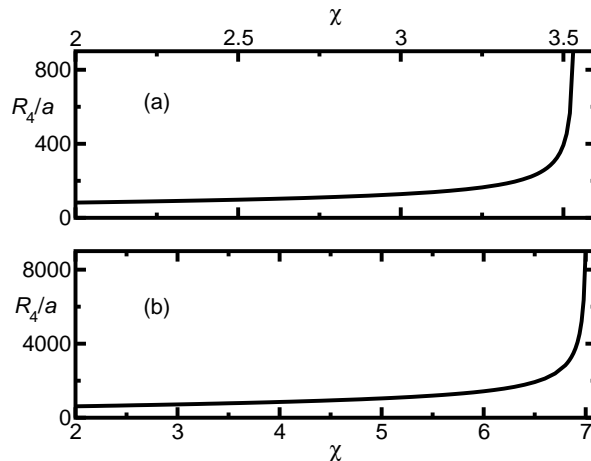


FIG. 7: Outer radius of the vesicle versus χ parameter for (a) $N_A = 100$, $N_B = 400$ and (b) $N_A = 1000$, $N_B = 13000$.

IV. CONCLUSIONS

Using a simple mean-field model, we have reproduced a number of features of the small, thick-walled vesicles formed in recent experiments^{2,3}. Our model predicts that the vesicles have a preferred radius for a range of parameters where the hydrophobic block is much longer than the hydrophilic block, agreeing with the experimental observation of a narrow vesicle size distribution in solutions of such polymers³. In our calculations, the origin of the free energy minimum that leads to the existence of a preferred radius is found to be a competition between the free energy of mixing of the solvent with the copolymers in the vesicle and the surface free energy of the vesicle. For asymmetric polymers with a long hydrophobic block, these terms are finely balanced, and a minimum in the free energy as a function of the vesicle radius appears. If the hydrophobic block is shortened, the minimum disappears, and the

vesicles become unstable with respect to the formation of smaller structures; i.e., spherical micelles. If, on the other hand, the hydrophobic block is lengthened, the free energy becomes a monotonically decreasing function of the vesicle radius, so that the vesicles no longer have a preferred size and may be, as in the experiments, unstable with respect to further aggregation. We also find that this instability may be triggered by a change in the interaction of the vesicles with the surrounding solvent. This raises the possibility of vesicles that burst, perhaps releasing an encapsulated cargo, when they move into a particular chemical environment.

Several extensions to our work are possible. Firstly, more realistic model parameters, and/or the use of different χ parameters for the A-block/B-block, A-block/solvent and B-block/solvent interactions, might improve the agreement of our theory with experimental results. In particular, our model predicts an initial slow growth of the vesicle radius as a function of N_B that accelerates gradually as the instability is approached. This is not in complete agreement with the experimental results², where the radius of the aggregates remains essentially constant over a range of N_B before increasing sharply at the instability. In addition, interdigitation of the molecules could be incorporated in a modified theory to allow the modelling of a wider range of systems. Finally, the model could also be applied to other copolymer architectures. For example, it should be able to describe the vesicles formed by triblock copolymers, such as Pluronic. The walls of these unilamellar vesicles²⁴ consist of three distinct layers (two outer hydrophilic layers and an inner hydrophobic layer), which could be modelled by the current approach.

-
- ¹ I. W. Hamley, *Block Copolymers in Solution: Fundamentals and Applications* (Wiley, Chichester, 2005).
- ² M. J. Derry, L. A. Fielding, N. J. Warren, C. J. Mable, A. J. Smith, O. O. Mykhaylyk, and S. P. Armes, *Chem. Sci.* **7**, 5078 (2016).
- ³ N. J. Warren, O. O. Mykhaylyk, A. J. Ryan, M. Williams, T. Doussineau, P. Dugourd, R. Antoine, G. Portale, and S. P. Armes, *J. Am. Chem. Soc.* **137**, 1929 (2014).
- ⁴ R. Lund, L. Willner, P. Lindner, and D. Richter, *Macromolecules* **42**, 2686 (2009).
- ⁵ L. Leibler, H. Orland, and J. C. Wheeler, *J. Chem. Phys.* **79**, 3550 (1983).
- ⁶ B. D. Simons and M. E. Cates, *J. Phys. II France* **2**, 1439 (1992).
- ⁷ B. A. Coldren, H. Warriner, R. van Zanten, J. A. Zasadzinski, and E. B. Sirota, *Langmuir* **22**, 2474 (2006).
- ⁸ S. Enders and D. Häntzschel, *Fluid Phase Equilib.* **153**, 1 (1998).
- ⁹ W. Li, H. Li, J. Li, H. Wang, H. Zhao, L. Zhang, Y. Xia, Z. Ye, J. Gao, J. Dai, et al., *Int. J. Nanomedicine* **7**, 4661 (2012).
- ¹⁰ D. C. Morse and S. T. Milner, *Phys. Rev. E* **52**, 5918 (1995).
- ¹¹ K. J. Storslett and S. J. Muller, *Biomicrofluidics* **11**, 034112 (2017).
- ¹² J. R. Howse, R. A. L. Jones, G. Battaglia, R. E. Ducker, G. J. Leggett, and A. J. Ryan, *Nat. Mater.* **8**, 507 (2009).
- ¹³ S. A. Safran, P. Pincus, and D. Andelman, *Science* **248**, 354 (1990).
- ¹⁴ J. Noolandi and K. M. Hong, *Macromolecules* **16**, 1443 (1983).
- ¹⁵ M. D. Whitmore and J. Noolandi, *Macromolecules* **18**, 657 (1985).
- ¹⁶ A. M. Mayes and M. O. de la Cruz, *Macromolecules* **21**, 2543 (1988).
- ¹⁷ M. R. Munch and A. P. Gast, *Macromolecules* **21**, 1360 (1988).
- ¹⁸ R.-J. Roe, *Macromolecules* **19**, 728 (1986).
- ¹⁹ P. G. de Gennes, *Macromolecules* **13**, 1069 (1980).
- ²⁰ E. Helfand and Y. Tagami, *J. Chem. Phys.* **56**, 3592 (1972).
- ²¹ R.-J. Roe and W.-C. Zin, *Macromolecules* **13**, 1221 (1980).
- ²² W. H. Press, S. A. Teukolsky, W. T. Vetterling, and B. P. Flannery, *Numerical Recipes* (Cambridge University Press, Cambridge, 2007), 3rd ed.
- ²³ W. Li, S. Liu, H. Yao, G. Liao, Z. Si, X. Gong, L. Ren, and L. Wang, *J. Colloid Interface Sci.* **508**, 145 (2017).
- ²⁴ T.-H. Kim, C. Song, Y.-S. Han, J.-D. Jang, and M. C. Choi, *Soft Matter* **10**, 484 (2014).